

Cavitation Erosion and Wet Environment Tribological Behaviour of Al₂O₃–13% TiO₂ Coatings Deposited via Different Atmospheric Plasma Spraying Parameters

M. SZALA^a, M. KAMIŃSKI^{b,*}, Ł. ŁATKA^c AND M. NOWAKOWSKA^c

^a*Department of Materials Engineering, Faculty of Mechanical Engineering, Lublin University of Technology, Nadbystrzycka 36, 20-618 Lublin, Poland*

^b*Department of Automotive Vehicles, Faculty of Mechanical Engineering, Lublin University of Technology, Nadbystrzycka 36, 20-618 Lublin, Poland*

^c*Faculty of Mechanical Engineering, Wrocław University of Science and Technology, Łukasiewicza 5, 50-371 Wrocław, Poland*

Doi: [10.12693/APhysPolA.142.733](https://doi.org/10.12693/APhysPolA.142.733)

*e-mail: mariusz.kaminski@pollub.pl

Atmospheric plasma spraying is an up-to-date and systematically developed technology. One of the crucial ideas is injecting the sprayed feedstock powder internally or externally into the plasma arc. The spraying parameters affect the microstructure and properties of the coating, which is decisive for the operation performance of coatings and specific machine components. This paper investigates the effect of atmospheric plasma spraying parameters, namely the feedstock injection mode and the spray distance, on cavitation erosion and wet environment tribological behaviour of Al₂O₃–13% TiO₂ coatings. The internal and external injection spraying mode, constant spray velocity (500 mm/s), and two spray distances to the substrate, namely 80 mm and 100 mm, were employed. The microstructure, porosity and hardness of the deposited coatings were studied. Cavitation erosion resistance was estimated using the ASTM G32 method. The sliding wear resistance has been estimated in the distilled water environment using the ball-on-disc apparatus. The results indicate that the internal injection supports the cavitation erosion resistance and the aquatic sliding wear. The coating fabricated with the 80 mm spray distance using the internal method is characterized by the smallest wear and the highest anti-erosion performance. A shorter spraying distance indicates greater coatings uniformity, while the increasing distance reduces the hardness and porosity, which are beneficial for the performance of the coatings. The main wet sliding wear mechanism has been fatigue-induced material detachment, while the cavitation erosion mechanism depends on the brittle fracture resulting in material detachment and pitting.

topics: tribology, cavitation erosion, microstructure, alumina–titania

1. Introduction

Atmospheric plasma spraying (APS) is an up-to-date and systematically developed technology. The conventional APS enables the deposition of coatings mainly from ceramics [1], metals [2], or composite [3] materials. This method usually injects the feedstock powder directly into the plasma jet, i.e., the external injecting mode. The essential modifications of conventional APS are injecting the sprayed feedstock powder internally into the plasma jet and providing the deposited material in the form of liquids (usually water-based suspension). These ideas are currently studied for different thermal spray methods, both APS [4, 5] and high-velocity oxygen fuel spraying (HVOF) [6, 7]. Changing the solid to liquid feedstock materials modifies conventional methods to novel processes named suspension plasma spraying (SPS) and suspension high-velocity oxygen fuel spraying (S-HVOF) [8, 9]. Besides the APS, spraying parameters affect the microstructure

and properties of the coating, which is decisive for the operation performance of coatings in specific applications [10, 11]. The literature presents the typical operational performance of ceramics evaluated under dry sliding wear conditions [12, 13]. However, as far as the authors' knowledge is concerned, there is no report on the water environment sliding wear of Al₂O₃–13% TiO₂ (AT13) coatings. Similarly, the knowledge about the cavitation erosion (CE) resistance of this type of coatings is presented mainly for the conventional APS with external feedstock injection mode [14, 15], while the cavitation performance of internal injection Al₂O₃–13% TiO₂ coatings have not been investigated yet.

Furthermore, there are scientific reports systematically broadening the knowledge about the dry sliding wear mechanism of ceramic coatings [16, 17], but there are no paper reports on the wet environment tribological behaviour of the APS Al₂O₃–13% TiO₂ coatings. Moreover, this research investigates the effect of the injecting mode on the wet sliding

wear resistance and combines the results with the cavitation erosion performance of coatings. However, this attempt has not been clarified in the literature yet. Finally, the papers reported in the literature examined the effect of APS deposition parameters on the cavitation erosion resistance and combined it with the microstructure and properties of the coating [18, 19]. However, there is no paper that clarifies the effect of injection mode on the cavitation erosion of Al_2O_3 -13% TiO_2 coatings. Therefore, this is a preliminary study discussing the effect of external and internal feedstock powder injection into the plasma on the cavitation erosion behaviour of the ceramic coating.

This paper investigates the effect of atmospheric plasma spraying parameters, namely the feedstock injection mode and the spraying distance, on the cavitation erosion and the wet environment tribological behaviour of the Al_2O_3 -13% TiO_2 coatings. Moreover, the wet environment sliding wear behaviour and the cavitation erosion performance were also analysed.

2. Materials and methods

The APS method was used for the deposition of alumina-titania (Al_2O_3 -13% TiO_2) coatings on the sand-blasted X5CrNi10-10 stainless steel substrate. The external and internal injection spraying mode, constant spray velocity (500 mm/s), and two spray distances to the substrate, namely 80 mm and 100 mm, were employed. The samples created using the external injection spraying mode are denoted, depending on the spray distance, as E-80 and E-100, and the ones created using the internal injection spraying mode as I-80 and I-100. In addition, the commercial feedstock powder Al_2O_3 + 13 wt% TiO_2 (Metco 6221, Oerlikon Metco, Switzerland) was used. The robotized setup was equipped with the SG-100 plasma torch, which was used for the coatings deposition and presented in detail in our previous paper [20]. It should be stressed that this torch is conventionally used for the APS external injection mode, and the setup rig was specially modified to allow internal injection. The specimen codes and crucial spray parameters are given in Table I.

The coating topographies, as well as the microstructure of cross-sections, were investigated with a scanning electron microscope (SEM) (Phenom-World, Eindhoven, The Netherlands). SEM micrographs were used to determine coatings thickness (magnification 500 \times) and for porosity evaluation (magnification 1000 \times). For each test, ten measurements were performed in random locations. The porosity was calculated according to the standard ASTM E2109-01 test method [21]. The average values, as well as the standard deviations, were calculated. The coatings hardness was measured with the Vickers indentation under the load of 1.96 N (HV0.2) and 10 s dwelling time using the HV-1000 hardness tester (Sinowon Innovation

TABLE I

The sample code and variable APS process parameters.

Sample code	Feedstock powder injection mode	Stand-off distance h [mm]	Relative torch scan speed V [mm/s]
E-80	external	80	500
E-100	external	100	
I-80	internal	80	
I-100	internal	100	

Metrology, DongGuan, China) according to the EN ISO 4516 standard [22]. For each coating, 10 indentations at the coating cross-section were made, and the average values, as well as the standard deviations, were calculated.

Utilized for tribological and cavitation erosion testing, the coatings were ground to achieve the $Ra \leq 0.16 \mu\text{m}$, $Rt \leq 4.45 \mu\text{m}$, and $RSm \leq 0.061 \text{ mm}$ surface roughness. The tribological tests were carried out by the ball-on-disc method in the aqueous environment (distilled water) using the Anton Paar Nanotribometer NTR2+. The tungsten carbide (WC) counter-sample (ball) with a diameter of 0.5 mm was used, and a load of 1.0 N was applied to it. The APS-coated sample was rotated at 90 RPM (3.77 cm/s), with a friction radius of 4 mm. During the test, the sliding distance was 2000 m each time. As a result of the tribological test, a wear track was formed on the sample surface, which was measured with the Taylor Hobson Intra contact profilometer in the xy plane. The tip radius of the measuring needle was 2 μm . The measurement involved making 401 profilograms at an interval of 5 μm , from which the surface topography map was generated, including a randomly selected fragment of the wear track. The material loss of the samples was evaluated based on the results of the profilometric measurements. The wear track cross-sectional area was used for the wear factor determination in compliance with the formula given in [14]. Finally, the sliding wear mechanism of the coatings was investigated and comparatively studied via the scanning electron microscope (Phenom-World, Eindhoven, The Netherlands).

Cavitation erosion was generated by the magnetostrictive-driven apparatus, resonating at 20 kHz with the peak-to-peak displacement amplitude of 50 μm described previously [23]. The apparatus was compliant with the ASTM G32 standard [24], and the measurements were performed by the stationary specimen method. The stand-off distance between the sonotrode-tip and the specimen surface was set to be equal to $1 \pm 0.05 \text{ mm}$. Distilled water was the testing medium. During the specific time intervals, the mass loss was estimated with an accuracy of 0.01 mg. Therefore, the cumulative mass loss and

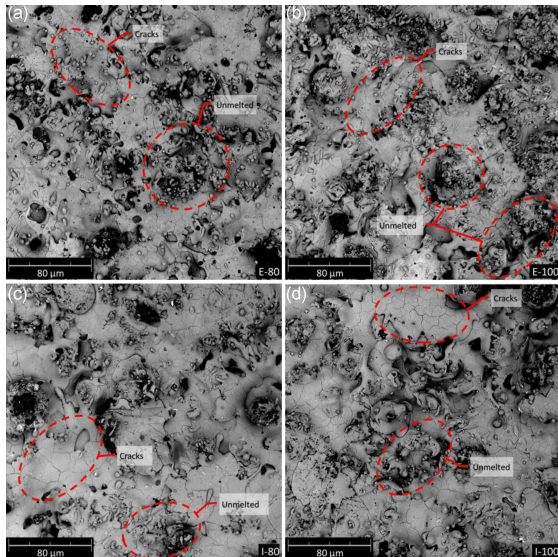


Fig. 1. As-sprayed coatings surface morphology (SEM image).

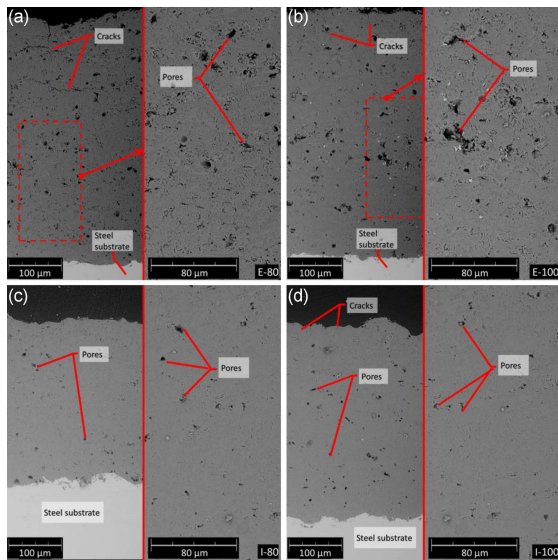


Fig. 2. Comparison of SEM images with different magnifications for coatings cross-section microstructures.

erosion time-rate curves were plotted for the total test time of 4 h. Eroded surfaces were analysed using a surface profiler (Surtronic S128, Taylor Hobson, Leicester, UK) and the SEM microscope to determine the cavitation erosion mechanism.

3. Results and discussion

3.1. Microstructure and properties

Generally, the spray parameters do not seriously affect the surface morphology (Fig. 1). Naturally, the splat-like morphology of the deposited Al_2O_3 -13% TiO_2 material is created for APS spraying,

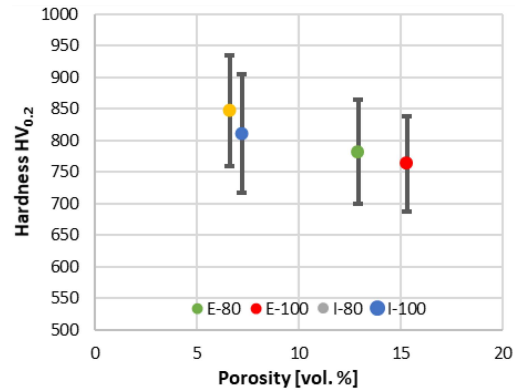


Fig. 3. Relationship between the coatings porosity and the Vickers hardness.

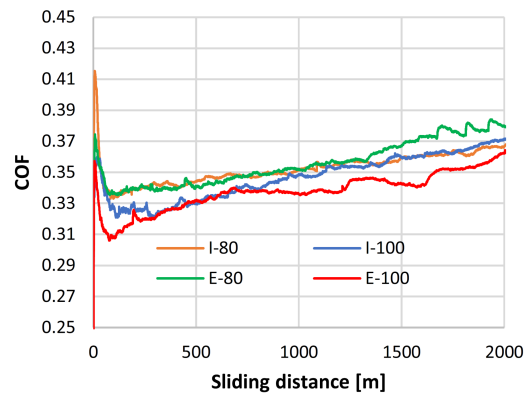


Fig. 4. Coefficient of friction variations estimated for the Al_2O_3 -13% TiO_2 (AT13) coatings tested in the water environment.

which is comparable to those reported by the literature [23, 25]. Moreover, surface oxidation, open porosity, not completely melted solid material particles, and cracks can be found. The external injection results in a much higher rate of unmelted and/or untreated powder particles, which are only sintered to the splats. This morphology could result in worse cohesion, which is very important for wear and cavitation erosion resistance issues. Even though the surfaces of the coatings are comparable to each other in terms of surface structure, their cross-microstructure differs (see Fig. 2). The comparative cross-section analysis confirms the impact of the spraying parameters on the microstructure of the coatings. All coatings show lamellar microstructure and sufficient bonding with the steel substrate. Some cracks were observed. Moreover, the different porosity and cracks ratio affects the hardness of the coatings (Fig. 3). All of these features can be explained by the variations in spray parameters. Generally, the hardness increases with the decreasing porosity of the coatings. The internal injection mode provides a much denser structure and larger hardness than the conventional external mode of APS deposition.

3.2. Tribological and cavitation erosion performance

Tribological performance has been investigated in the wet environment. The analysis of coefficient of friction (COF) (Fig. 4) and wear rates (Fig. 5) suggests lower COF and wear rates than those reported in the literature [14]. The water environment seems to decrease material loss by minimizing friction. Therefore the friction coefficient has lower values than those reported for the dry sliding wear testing of alumina–titania coatings. The wear results indicate the effect of spray parameters. The coatings sprayed with a shorter distance, i.e., 80 mm, are characterized by smaller wear. In particular, the internal injection mode results in the smallest material loss and shallow wear track (see Fig. 6). The analysis of the SEM photos of worn surfaces confirms that the wear mechanism of APS sprayed coatings tested in a wet sliding environment shows a fatigue nature (see Fig. 7). The fatigue action is confirmed by the presence of cracks perpendicular to the sliding direction. These cracks result from cyclic compressing of the coating material with the sliding action of the counterball. Then the cracked materials undergo spallation and removal. Pores and surface nonuniformities are the centres of cracking and accelerate material loss. The wet environment sliding wear mechanism differs from those reported for the dry sliding conditions [14]. Secondary mechanisms, such as adhesive smearing of abrasive wear products, have not been reported in this experiment.

The cavitation curves shown in Fig. 8 confirm that the spray distance affects the erosion results. The coatings sprayed at shorter distances present better erosion resistance. Moreover, it seems that the internal injection supports the anti-cavitation performance too. Therefore the highest erosion resistance was noticed for the I-80 coating. Generally, mass losses for all tested coatings (Fig. 8a) are comparable to those presented in our previous studies for ceramics tested under similar cavitation conditions [6, 14]. The cavitation erosion rates (Fig. 8b) indicate lower wear rates of I-80 and E-80 coatings which are related to the microstructural differences of the coatings.

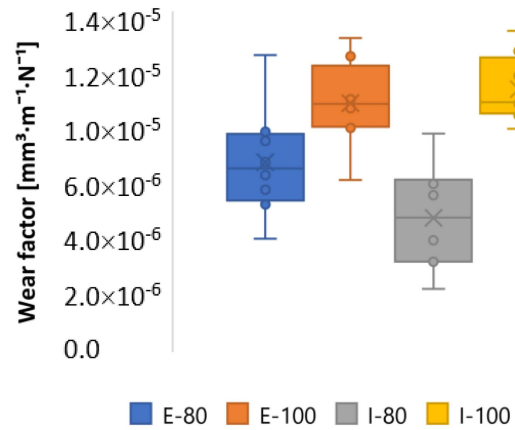


Fig. 5. Wear factor of the tested coatings.

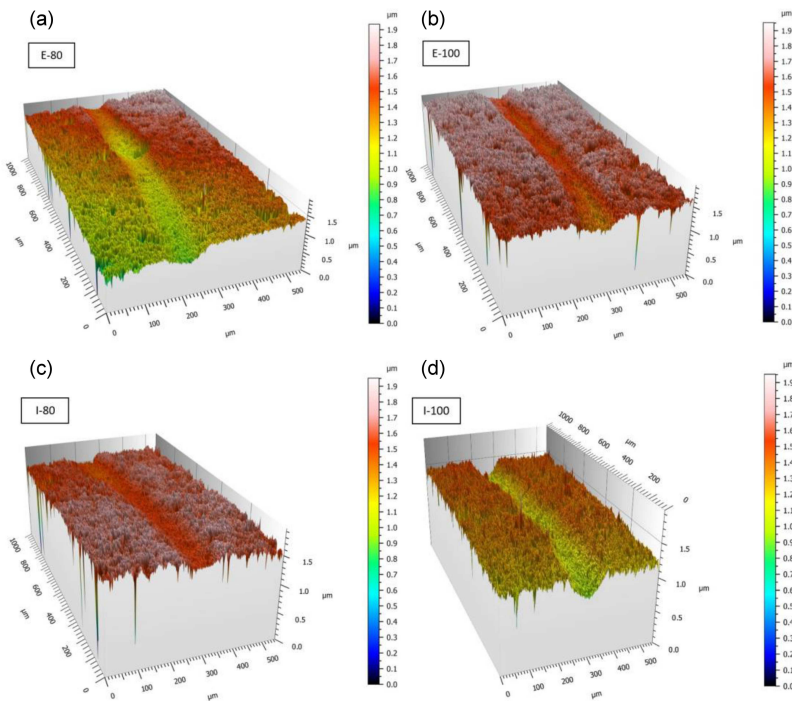


Fig. 6. Topography of the wear tracks of E-80, E-100, I-80, and I-100 samples.

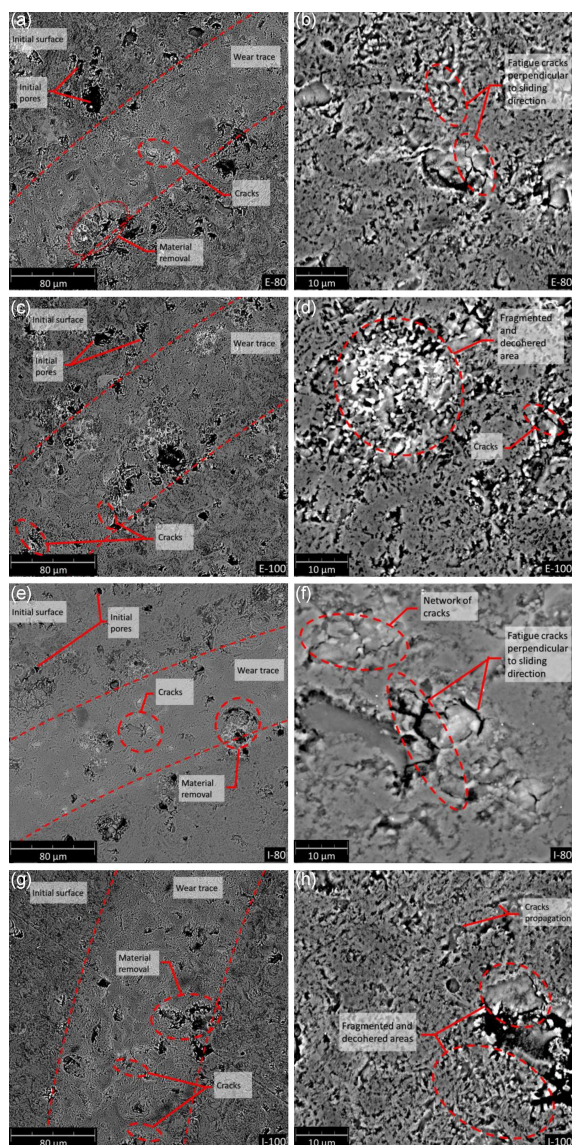


Fig. 7. Worn surfaces of Al_2O_3 -13% TiO_2 coatings tested in the water environment. Panels (a, c, e, h) present SEM surface overview, and panels (b, d, f, h) — SEM images of enlarged worn area.

The cavitation erosion mechanism of Al_2O_3 -13% TiO_2 coatings has a brittle nature. Thus, the presence of structure nonuniformities such as porosity, cracks, and unmelted particles initiates and further accelerates erosive damage (Figs. 9–12). Initially, cracks and decohered material particles are detached and removed. Then, pits and craters grow, and the removed material rate increases. The cavitation erosion relates to brittle cracking due to the cyclic action of cavitation loads. However, this overall cavitation erosion mechanism differs in the case of specific coating. The comparative analysis of the eroded surfaces (Figs. 9–12) allows us to identify differences in the surface structure of eroded coatings with those in the cavitation erosion mechanism. First, the coatings present a smaller mass loss and

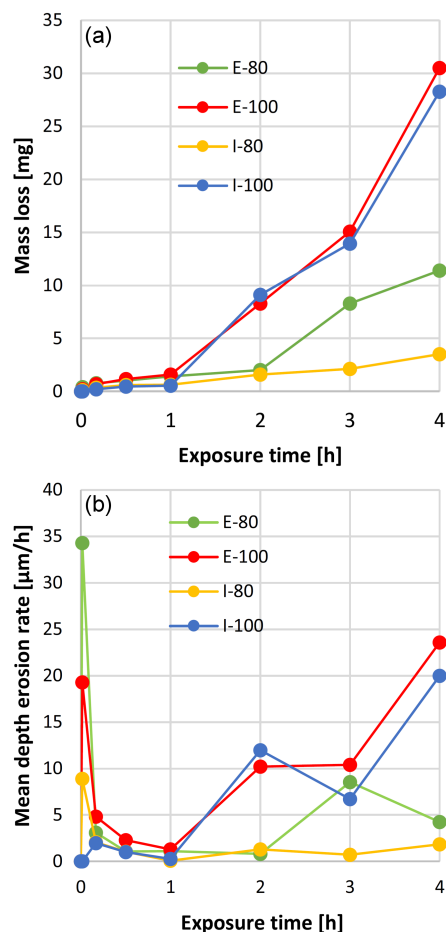


Fig. 8. Cavitation erosion mass loss and rate-time curves of AT13 coatings.

a larger CE resistance of I-80 or E-80 than seriously eroded E-100 and I-100. The analysis of the profilometric results shows that the external deposition results in deep pits while the internally deposited coatings show a much more uniform morphology of eroded surface (see the roughness results given in Table II). This is confirmed by the SEM analysis, which reveals the uneroded surface areas (Figs. 9–12). Contrary to that, severe surface damage and high roughness are observed for the severely damaged E-100 and I-100 coatings. Moreover, the feedstock spray mode seems to influence erosion kinetics. Therefore, the externally sprayed coatings material seems less coherent than those fabricated by the internal deposition. Eroded I-100 and I-80 seem less fragmented than their external equivalents. Erosion of externally deposited coatings relates to the fine particles detachment, while the internally deposited coatings show the chunk material detachment. A shorter spray distance allows the sprayed coating material to melt and densifies the coating structure. This improves the uniformity of the coating and facilitates anti-cavitation performance.

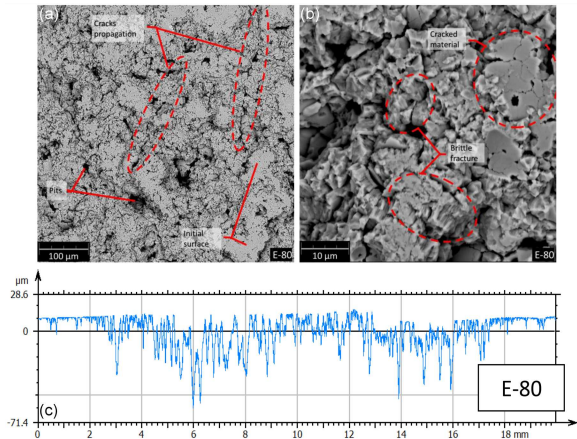


Fig. 9. Eroded surfaces SEM images (a–b) and surface profile (c) of E-80 AT13 coatings after 4 h of testing.

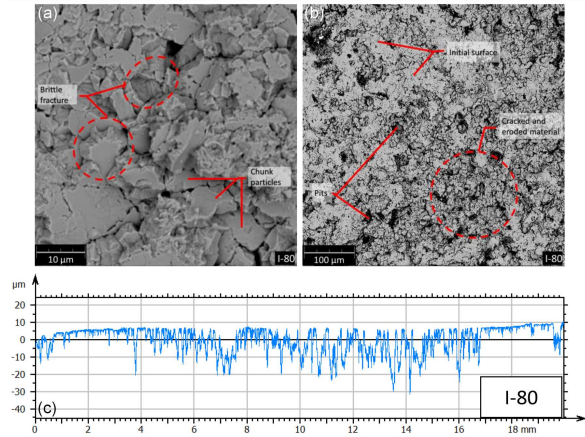


Fig. 11. Eroded surfaces SEM images (a–b) and surface profile (c) of I-80 AT13 coatings after 4 h of testing.

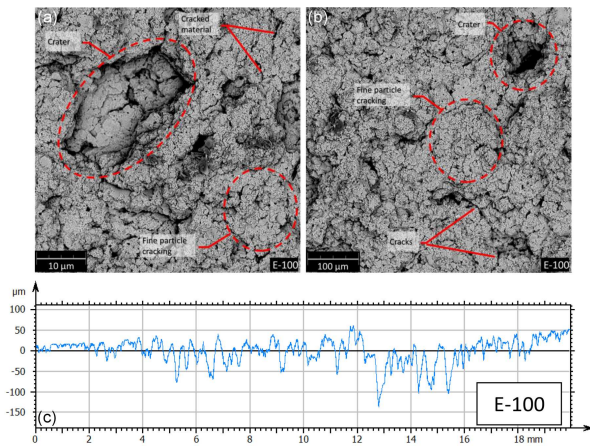


Fig. 10. Eroded surfaces SEM images (a–b) and surface profile (c) of E-100 AT13 coatings after 4 h of testing.

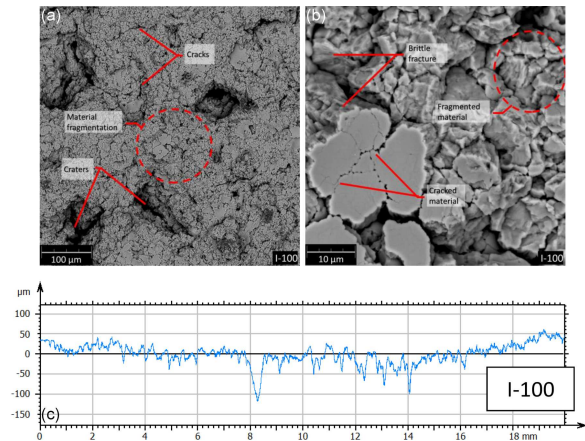


Fig. 12. Eroded surfaces SEM images (a–b) and surface profile (c) of I-100 AT13 coatings after 4 h of testing.

TABLE II

The surface roughness estimated after 4 h of cavitation testing and RR (roughness rate) parameter.

Coating	Surface roughness [μm]			RR [μm]
	RSm	Ra	Rt	
E-80	168	6.2	35.3	28.9
E-100	256	12.6	111.0	28.7
I-80	98	4.4	31.8	13.2
I-100	191	7.7	89.0	16.2

The cavitation eroded surface characterized by the profilometry measurements allows the combining of the roughness rate parameter (RR , see Table II) with the properties of the initial coating, such as hardness and porosity (see Fig. 2). The roughness rate (RR) proposed by M. Szala in [26] combines

the Ra , Rt , and RSm roughness parameters. This is useful for the surface morphology characterization of cavitation eroded surfaces of HVOF sprayed metallic coatings. The analysis of RR calculated for the APS sprayed Al_2O_3 –13% TiO_2 coatings confirms that porosity increases and the hardness decreases the RR parameter. According to our previous papers regarding the cavitation erosion resistance of coating materials [27–29], it seems evident that apart from porosity and hardness, other mechanical, physical, and microstructural factors affect the cavitation erosion behaviour. Therefore, considering hardness, porosity, and material factors, the overall relationship for APS sprayed Al_2O_3 –13% TiO_2 can be stated as

$$RR \simeq \frac{\text{porosity}}{\text{hardness}} \times \text{material factor.} \quad (1)$$

This relationship is helpful for the prediction of the morphology of the cavitation eroded surface and provides a promising idea for coatings erosion mechanism characterization. High porosity results in severe surface erosion and pitting, while lower porosity favours uniform erosion of coatings due to large coating toughness. However, this idea must be studied for a broader range of coatings.

The spray parameters determine hardness and porosity levels and affect the sprayed ceramics wear and cavitation erosion behaviour. Tougher and denser coatings show better anti-cavitation performance, which was proved by the comparative study carried out for the APS, SPS, and S-HVOF coatings [29]. In the case of wear resistance, hardness is a predominant factor that results in the anti-wear behaviour of the coatings. Finally, the complementary results were obtained for the cavitation erosion and wet sliding wear, i.e., the coatings characterized by high cavitation erosion resistance have better wear behaviour.

4. Conclusions

Considering the research results, it can be concluded that the properties of the atmospheric plasma sprayed ceramics are affected by the spray parameters. The following conclusions can be drawn.

- The internally deposited Al₂O₃-13% TiO₂ coatings show slightly higher microhardness values compared to the externally deposited coatings.
- The porosity of the internally deposited coatings is twice as low as that of the externally deposited coatings. Generally, the hardness increases with the decreasing porosity of coatings. The internal injection mode provides almost twice the denser structure and higher hardness than the external spray mode.
- The cavitation erosion resistance correlates well with the tribological results.
- The coating deposited internally, from the distance of 80 mm, turned out to be by far the most resistant to wear under wet wear conditions. A slight effect of the material feeding technique was demonstrated. For tribological wear, the distance from which the coating is deposited is definitely the most important.
- As a result of the tests for resistance to cavitation erosion, the coating deposited internally from a distance of 80 mm has also proved to be the most resistant. Similarly to the tribological test, a significant effect of the sample deposition distance was found in this case. The internal injection of the feedstock powder seems beneficial for the cavitation erosion resistance.
- The primary mechanism of wet sliding wear was fatigue, while cavitation erosion relates to brittle cracking due to the cyclic action of cavitation loads. The surface erosion mechanism correlates with the initial hardness and porosity.

Acknowledgments

The project/research was financed in the framework of the project Lublin University of Technology Regional Excellence Initiative, funded by the Polish Ministry of Science and Higher Education (contract no. 030/RID/2018/19).

References

- [1] J. Kiilakoski, R. Musalek, F. Lukac, H. Koivuluoto, P. Vuoristo, *J. Eur. Ceram. Soc.* **38**, 1908 (2018).
- [2] E. Hejrani, D. Sebold, W.J. Nowak, G. Mauer, D. Naumenko, R. Vaßen, W.J. Quadackers, *Surf. Coat. Technol.* **313**, 191 (2017).
- [3] M. Szala, A. Dudek, A. Maruszczczyk, M. Walczak, J. Chmiel, M. Kowal, *Acta Phys. Pol. A* **136**, 335 (2019).
- [4] L. Łatka, M. Michalak, E. Jonda, *Adv. Mater. Sci.* **19**, 5 (2019).
- [5] M. Michalak, F.-L. Toma, L. Łatka, P. Sokolowski, M. Barbosa, A. Ambroziak, *Materials* **13**, 2638 (2020).
- [6] M. Michalak, P. Sokołowski, M. Szala, M. Walczak, L. Łatka, F.-L. Toma, S. Björklund, *Coatings* **11**, 879 (2021).
- [7] A. Potthoff, R. Kratzsch, M. Barbosa, N. Kulissa, O. Kunze, F.-L. Toma, *J. Therm. Spray Tech.* **27**, 710 (2018).
- [8] L. Łatka, M. Szala, W. Macek, R. Branco, *Adv. Sci. Technol. Res. J.* **14**, 307 (2020).
- [9] F.-L. Toma, A. Potthoff, L.-M. Berger, C. Leyens, *J. Therm. Spray Tech.* **24**, 1143 (2015).
- [10] A. Góral, W. Żórawski, L. Lityńska-Dobrzyńska, *Mater. Charact.* **96**, 234 (2014).
- [11] S. Mehar, S.G. Sapate, N. Vashishtha, P. Bagde, *Ceram. Int.* **46**, 11799 (2020).
- [12] M. Öge, Y. Kucuk, M.S. Gok, A.C. Karaoglanli, *Int. J. Appl. Ceram. Technol.* **16**, 2283 (2019).
- [13] Y. Küçük, *J. Asian Ceram. Soc.* **9**, 237 (2021).
- [14] L. Łatka, M. Michalak, M. Szala, M. Walczak, P. Sokolowski, A. Ambroziak, *Surf. Coat. Technol.* **410**, 126979 (2021).

- [15] V. Matikainen, K. Niemi, H. Koivuluoto, P. Vuoristo, *Coatings* **4**, 18 (2014).
- [16] D. Kumar, Q. Murtaza, R.S. Walia, P. Singh, *Surf. Topogr. Metrol. Prop.* **10**, 015043 (2022).
- [17] P. Bagde, S.G. Sapate, R.K. Khatirkar, N. Vashishtha, *Tribol. Int.* **121**, 353 (2018).
- [18] K. Jafarzadeh, Z. Valefi, B. Ghavidel, *Surf. Coat. Technol.* **205**, 1850 (2010).
- [19] M. Szala, L. Łatka, M. Awtoniuk, M. Winnicki, M. Michalak, *Processes* **8**, 1544 (2020).
- [20] M. Michalak, L. Łatka, P. Sokołowski, A. Niemiec, A. Ambroziak, *Coatings* **10**, 173 (2020).
- [21] ASTM E2109-01, “Standard Test Methods for Determining Area Percentage Porosity in Thermal Sprayed Coatings”, ASTM International, 2010.
- [22] ISO 4516:2002, “Metallic and Other Inorganic Coatings — Vickers and Knoop Microhardness Tests”, 2002.
- [23] L. Łatka, M. Szala, M. Michalak, T. Pałka, *Acta Phys. Pol. A.* **136**, 342 (2019).
- [24] ASTM G32-10, “Standard Test Method for Cavitation Erosion Using Vibratory Apparatus”, ASTM International, West Conshohocken (PA) 2010.
- [25] J. Zhou, K. Sun, S. Huang, W. Cai, Y. Wei, L. Meng, Z. Hu, W. Li, *Coatings* **10**, 1122 (2020).
- [26] M. Szala, *Tribologia* **298**, 47 (2021).
- [27] M. Szala, M. Walczak, T. Hejwowski, *Adv. Sci. Technol. Res. J.* **15**, 376 (2021).
- [28] M. Szala, M. Walczak, A. Świetlicki, *Materials* **15**, 93 (2022).
- [29] M. Nowakowska, L. Łatka, P. Sokołowski, M. Szala, F.-L. Toma, M. Walczak, *Wear* **508–509**, 204462 (2022).